Topological Data Analysis —

A Role for Algebraic Topology in Analyzing Models and Data

Sarah Day
WM GAG Seminar
April 3, 2024

with Yu-Min Chung (Eli Lilly), Kait Keegan (UNR), Laura Storch (Bates), Sage Stanish (WM `22, Glasgow), Julius Kiewel (WM)

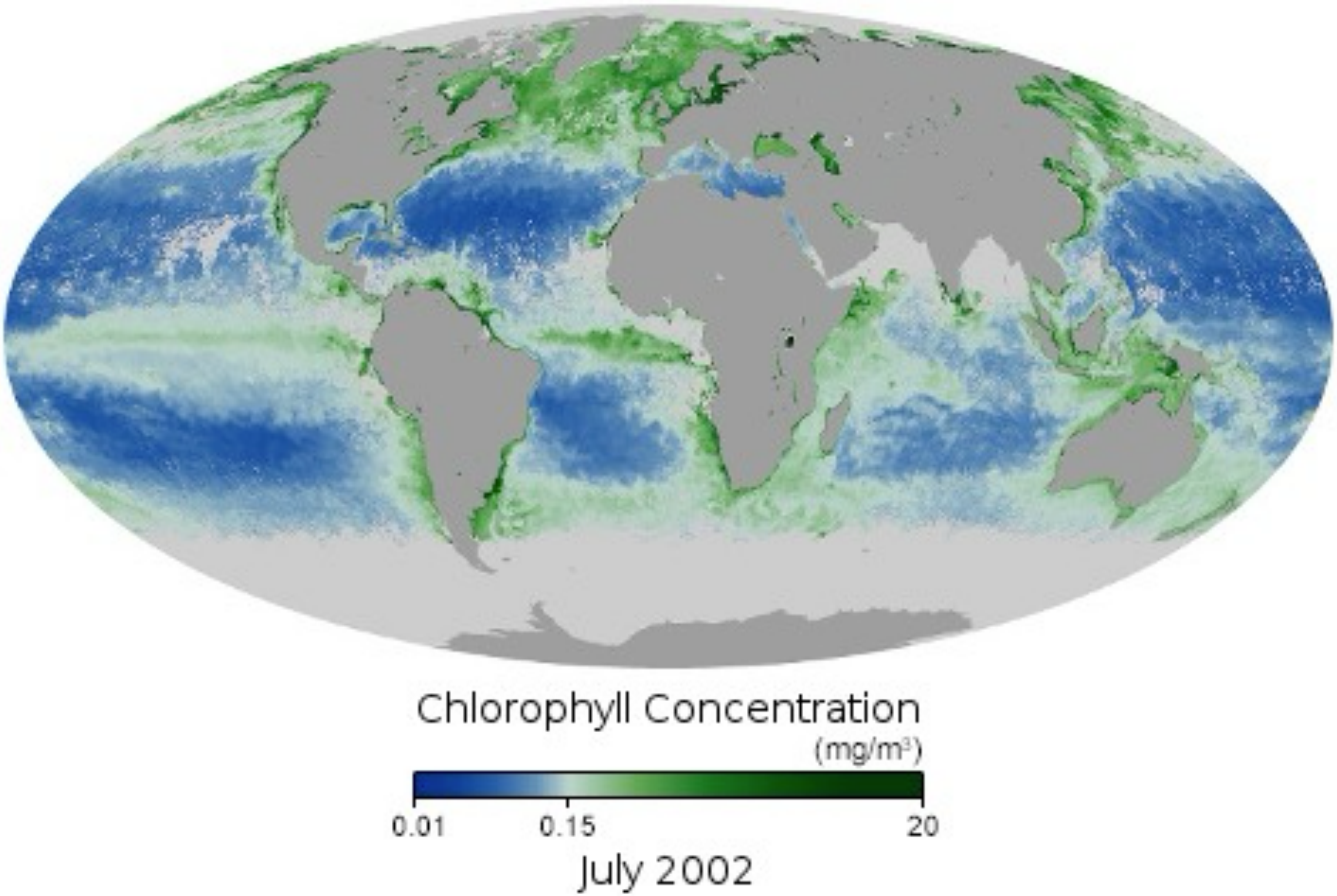

https://earthobservatory.nasa.gov/global-maps/MY1DMM_CHLORA

(Topology, Wikipedia)

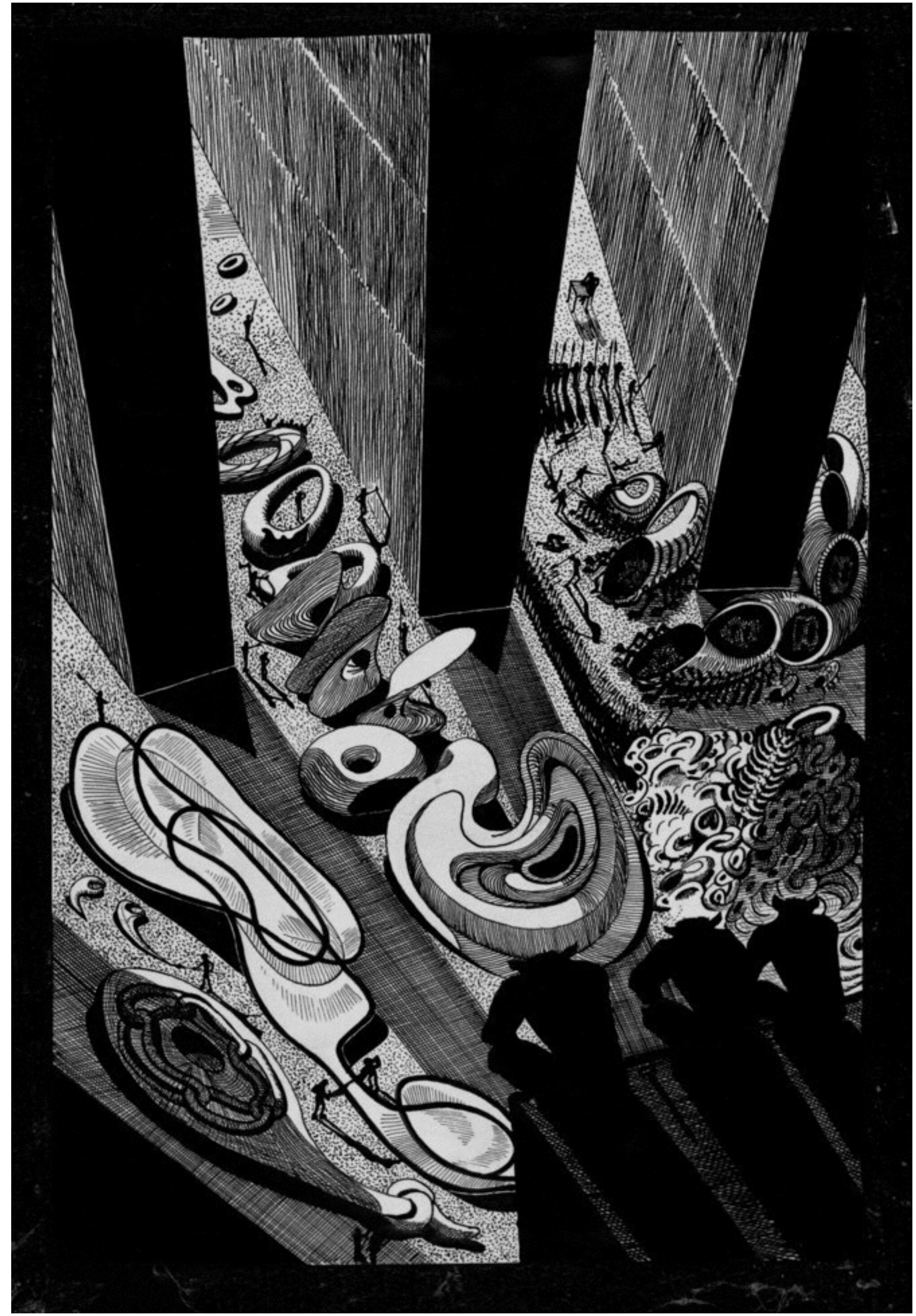

Topological Zoo
Anatoly Fomenko
1967

Homology

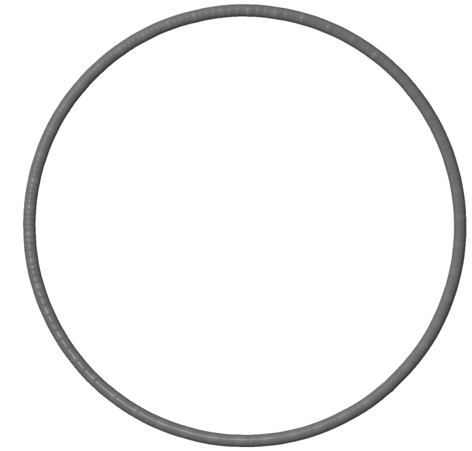

$$H_k(X) \cong \begin{cases} \mathbb{Z} & k = 0, 1 \\ 0 & \text{otherwise.} \end{cases}$$

$$H_k(S^n) \cong \begin{cases} \mathbb{Z} & k = 0, n \\ 0 & \text{otherwise.} \end{cases}$$

or

$$H_k(X) \cong \begin{cases} \mathbb{Z} & k = 0, 2 \\ \mathbb{Z}^2 & k = 1 \\ 0 & \text{otherwise.} \end{cases}$$

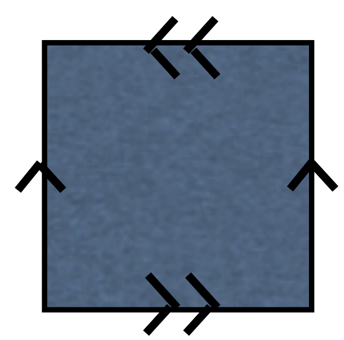

$$H_k(K) \cong \begin{cases} \mathbb{Z} & k = 0, \\ \mathbb{Z} \oplus \mathbb{Z}/2\mathbb{Z} & k = 1, \\ 0 & \text{otherwise.} \end{cases}$$

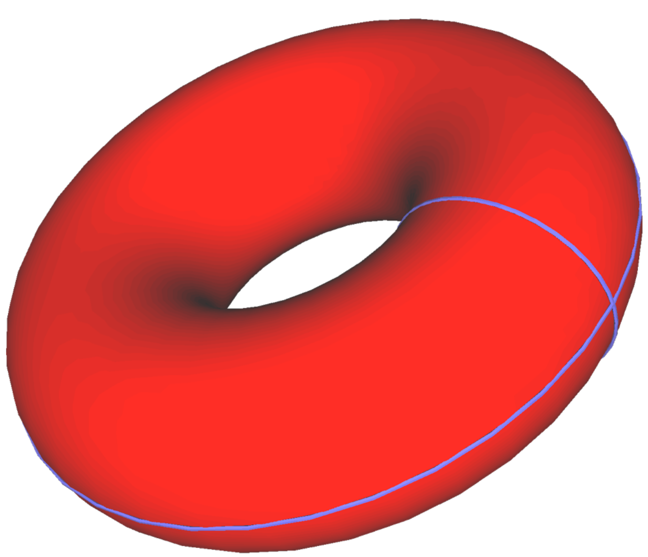

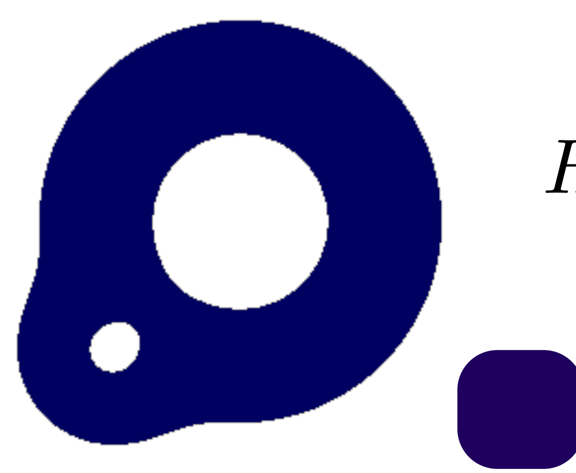

$$H_k(X) \cong \begin{cases} \mathbb{Z}^2 & k = 0, 1 \\ 0 & \text{otherwise.} \end{cases}$$

Betti numbers

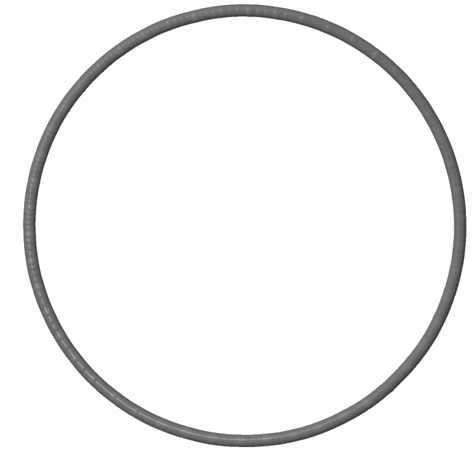

$$H_k(X) \cong \begin{cases} \mathbb{Z} & k = 0, 1 \\ 0 & \text{otherwise.} \end{cases}$$

$$\beta_0 = 1$$
$$\beta_1 = 1$$

or

$$\beta_0 = 1$$
$$\beta_1 = 2$$
$$\beta_2 = 1$$

$$H_k(X) \cong \begin{cases} \mathbb{Z} & k = 0, 2 \\ \mathbb{Z}^2 & k = 1 \\ 0 & \text{otherwise.} \end{cases}$$

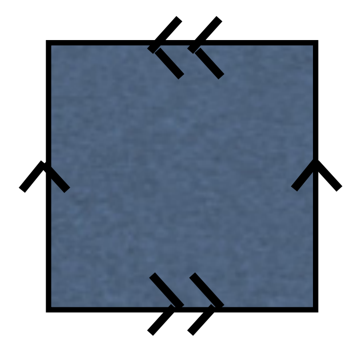

$$H_k(K) \cong \begin{cases} \mathbb{Z} & k = 0, \\ \mathbb{Z} \oplus \mathbb{Z}/2\mathbb{Z} & k = 1, \\ 0 & \text{otherwise.} \end{cases}$$

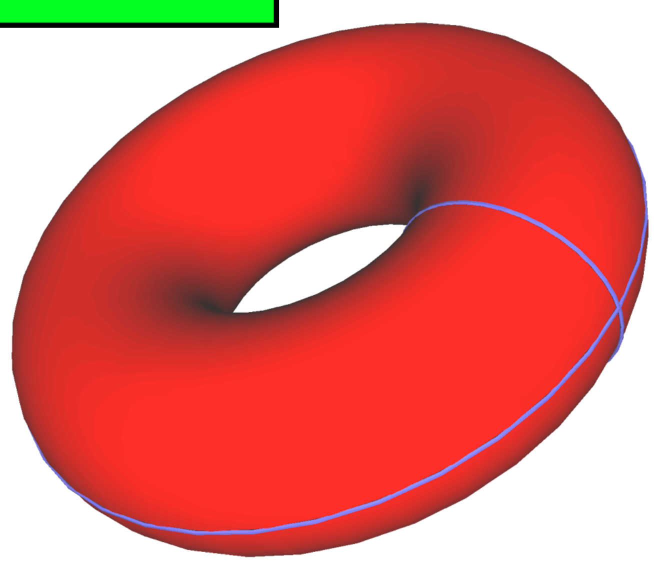

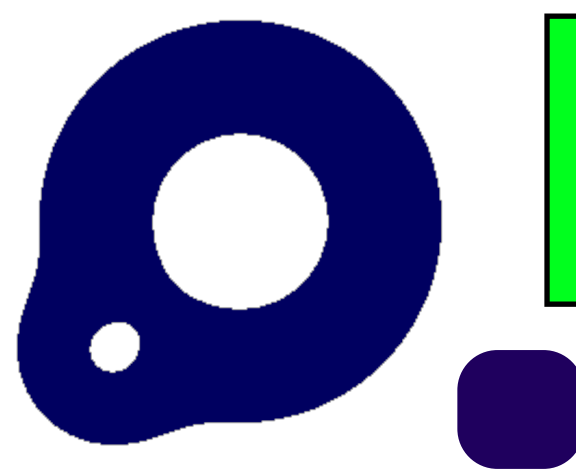

$$\beta_0 = 2$$
$$\beta_1 = 2$$

$$H_k(X) \cong \begin{cases} \mathbb{Z}^2 & k = 0, 1 \\ 0 & \text{otherwise.} \end{cases}$$

Betti numbers and Euler Characteristic

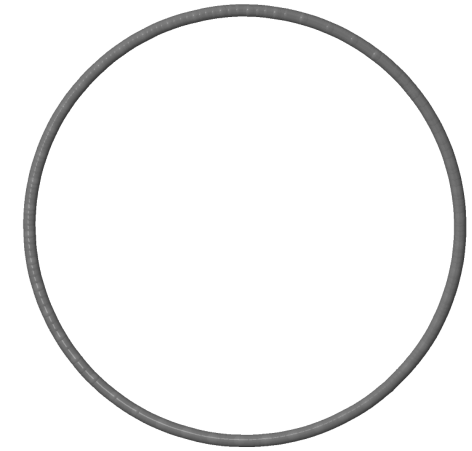

$$H_k(X) \cong \begin{cases} \mathbb{Z} & k = 0, 1 \\ 0 & \text{otherwise.} \end{cases}$$

$\beta_0 = 1$

$\beta_1 = 1$

$$\chi = \sum (-1)^n k_n = \sum (-1)^n \beta_n$$

or

$\beta_0 = 1$

$\beta_1 = 2$

$\beta_2 = 1$

$$H_k(X) \cong \begin{cases} \mathbb{Z} & k = 0, 2 \\ \mathbb{Z}^2 & k = 1 \\ 0 & \text{otherwise.} \end{cases}$$

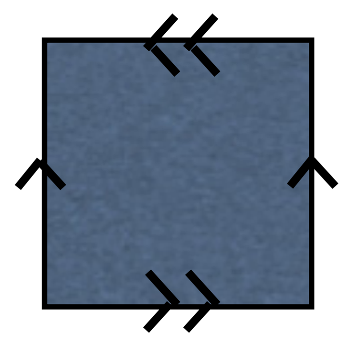

$$H_k(K) \cong \begin{cases} \mathbb{Z} & k = 0, \\ \mathbb{Z} \oplus \mathbb{Z}/2\mathbb{Z} & k = 1, \\ 0 & \text{otherwise.} \end{cases}$$

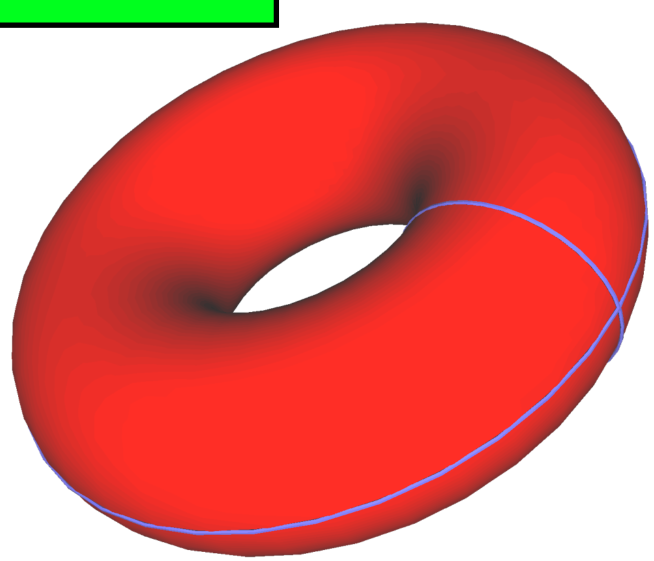

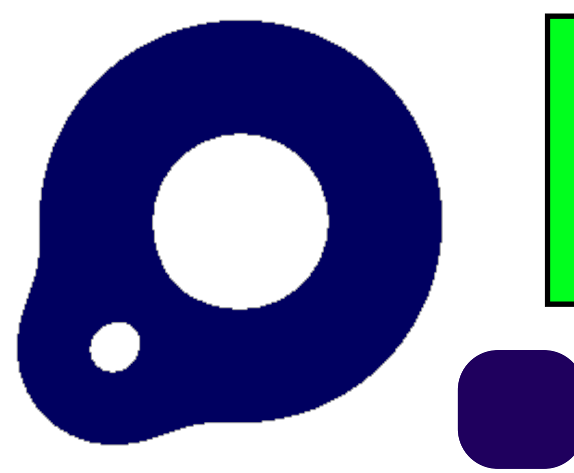

$\beta_0 = 2$

$\beta_1 = 2$

$$H_k(X) \cong \begin{cases} \mathbb{Z}^2 & k = 0, 1 \\ 0 & \text{otherwise.} \end{cases}$$

population density patterns

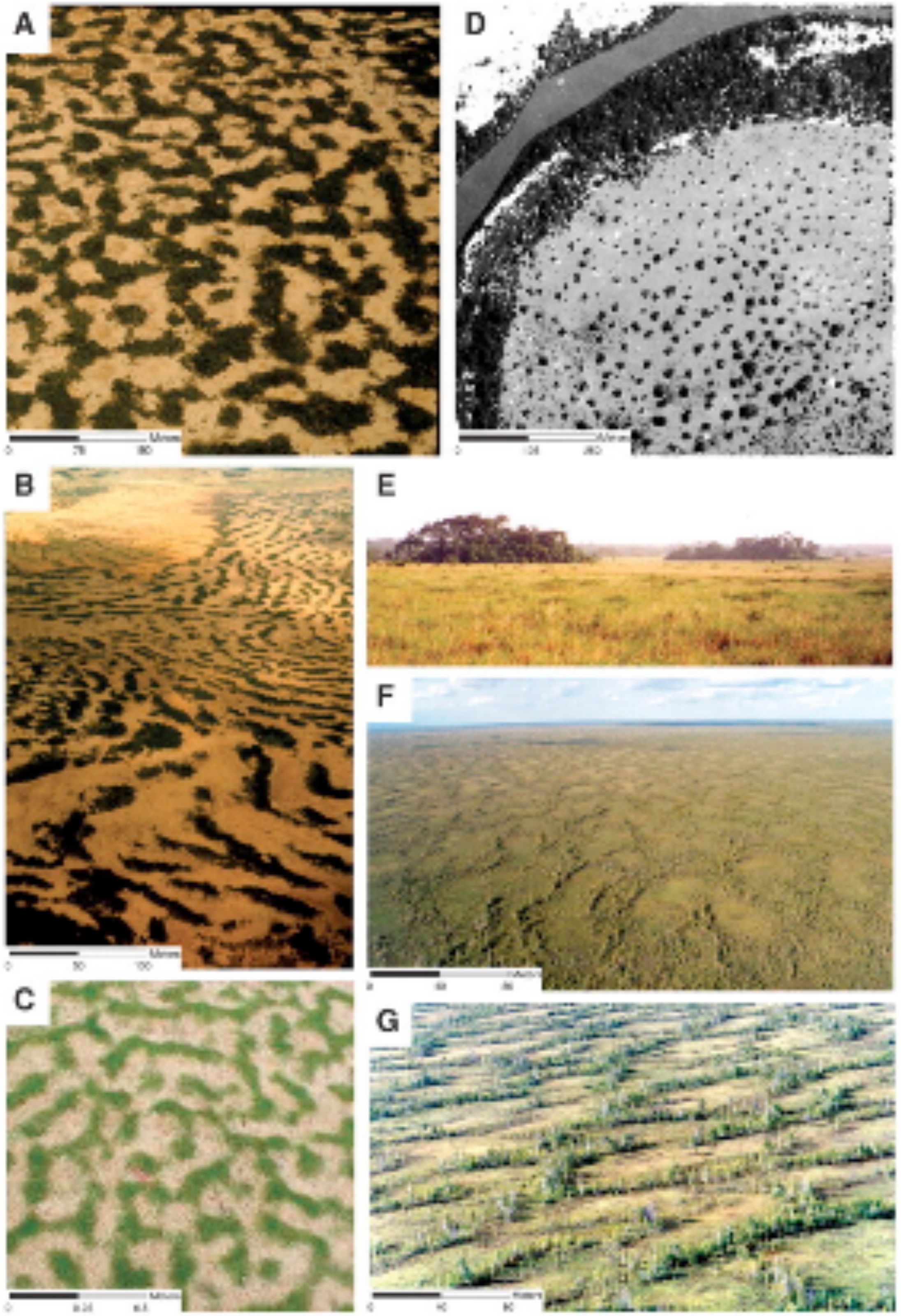

M Rietkerk et al. Science 2004;305:1926-1929

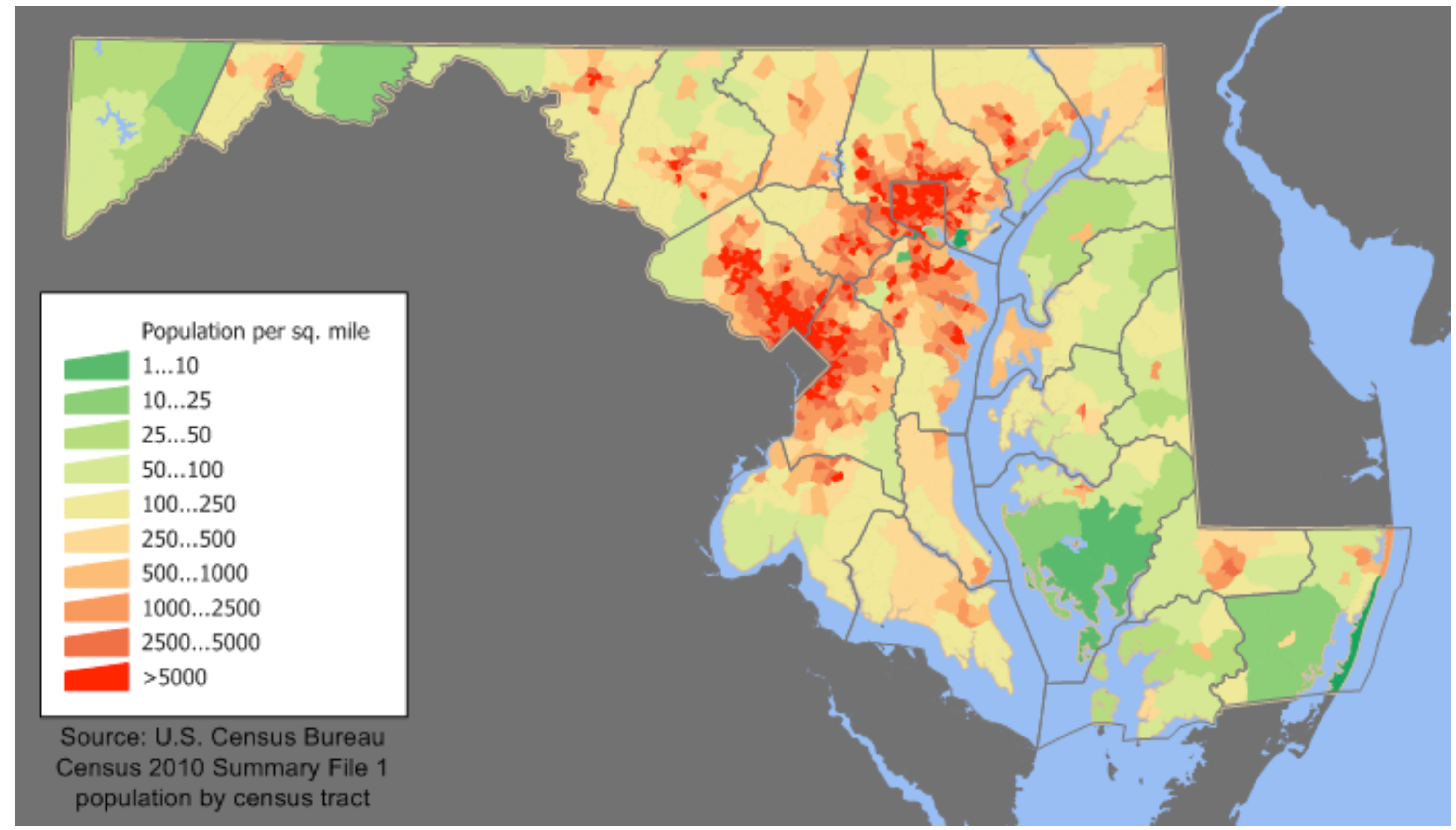

http://en.wikipedia.org/wiki/Maryland

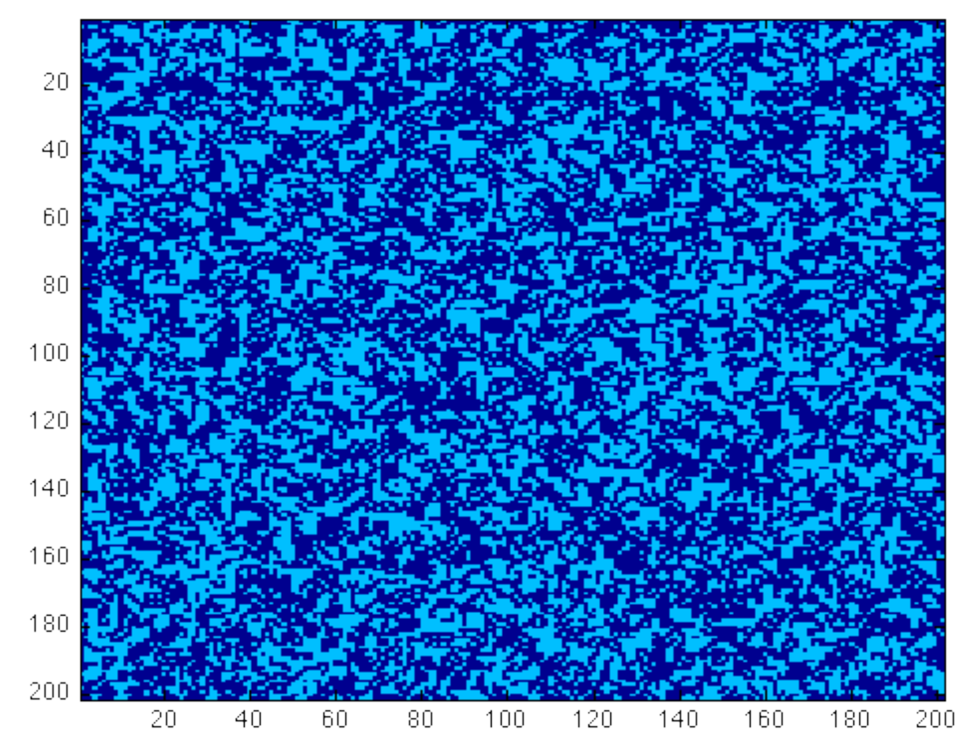

Coupled-patch growth/dispersal lattice model

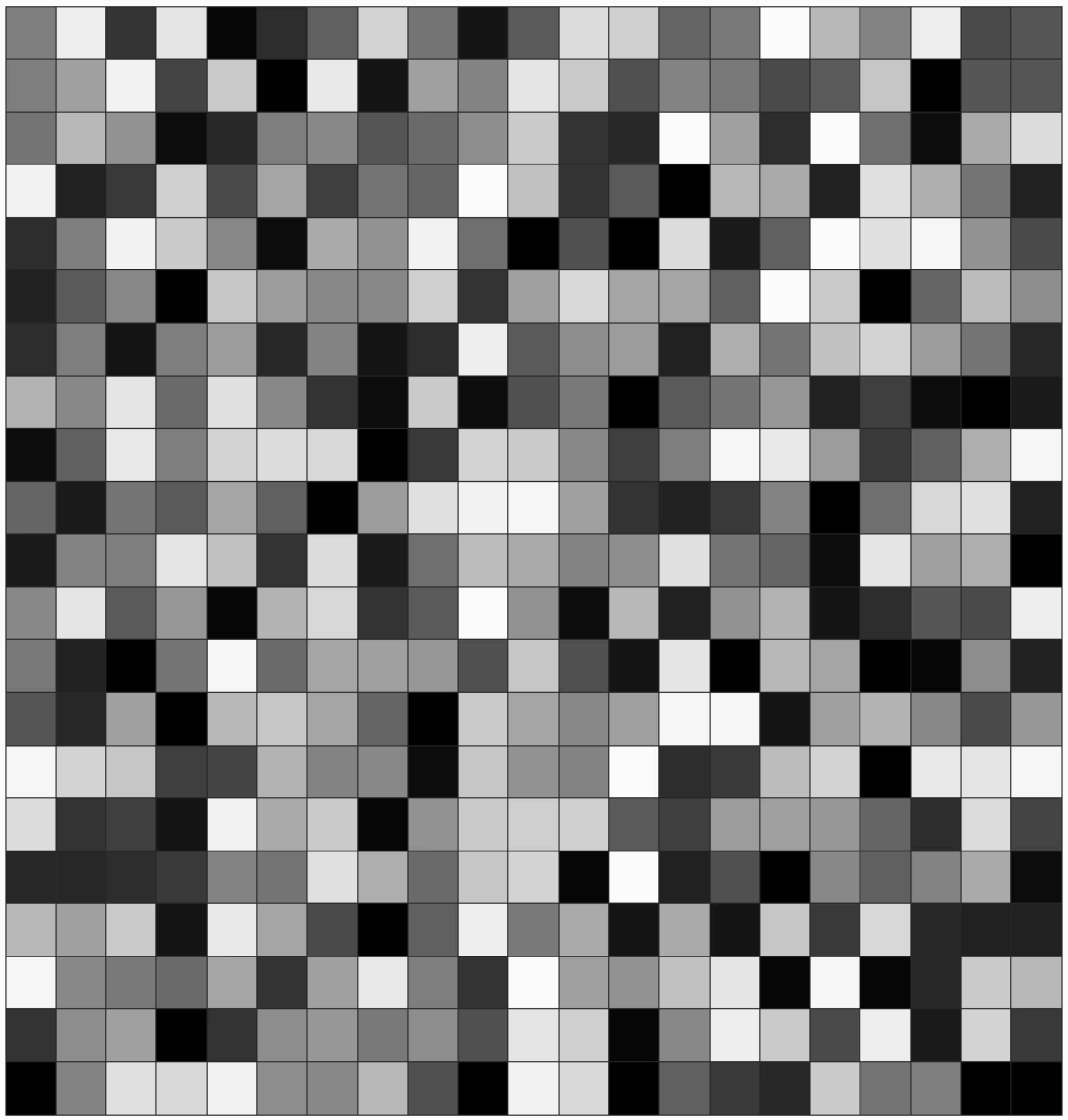

Low dispersal

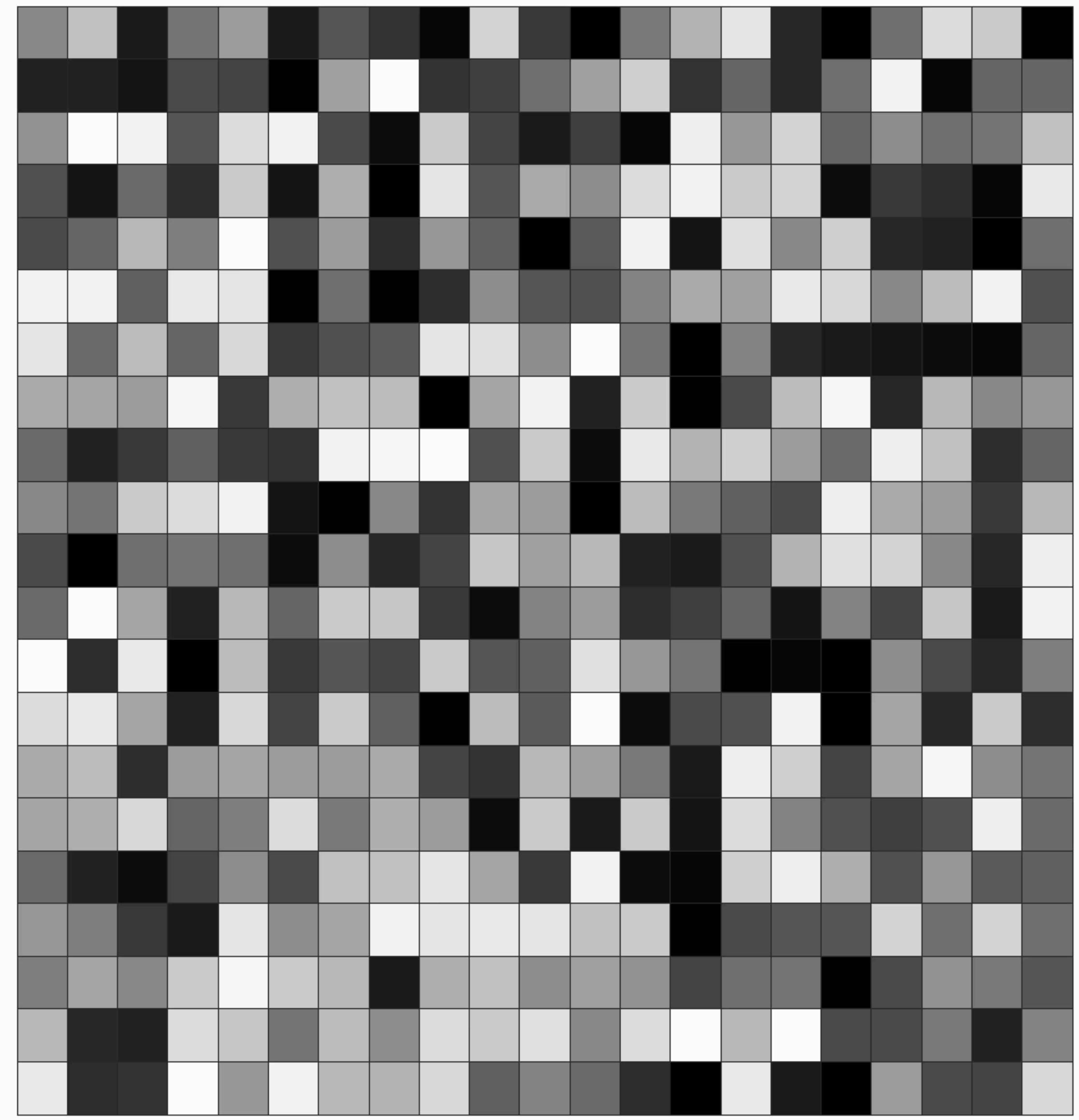

High dispersal

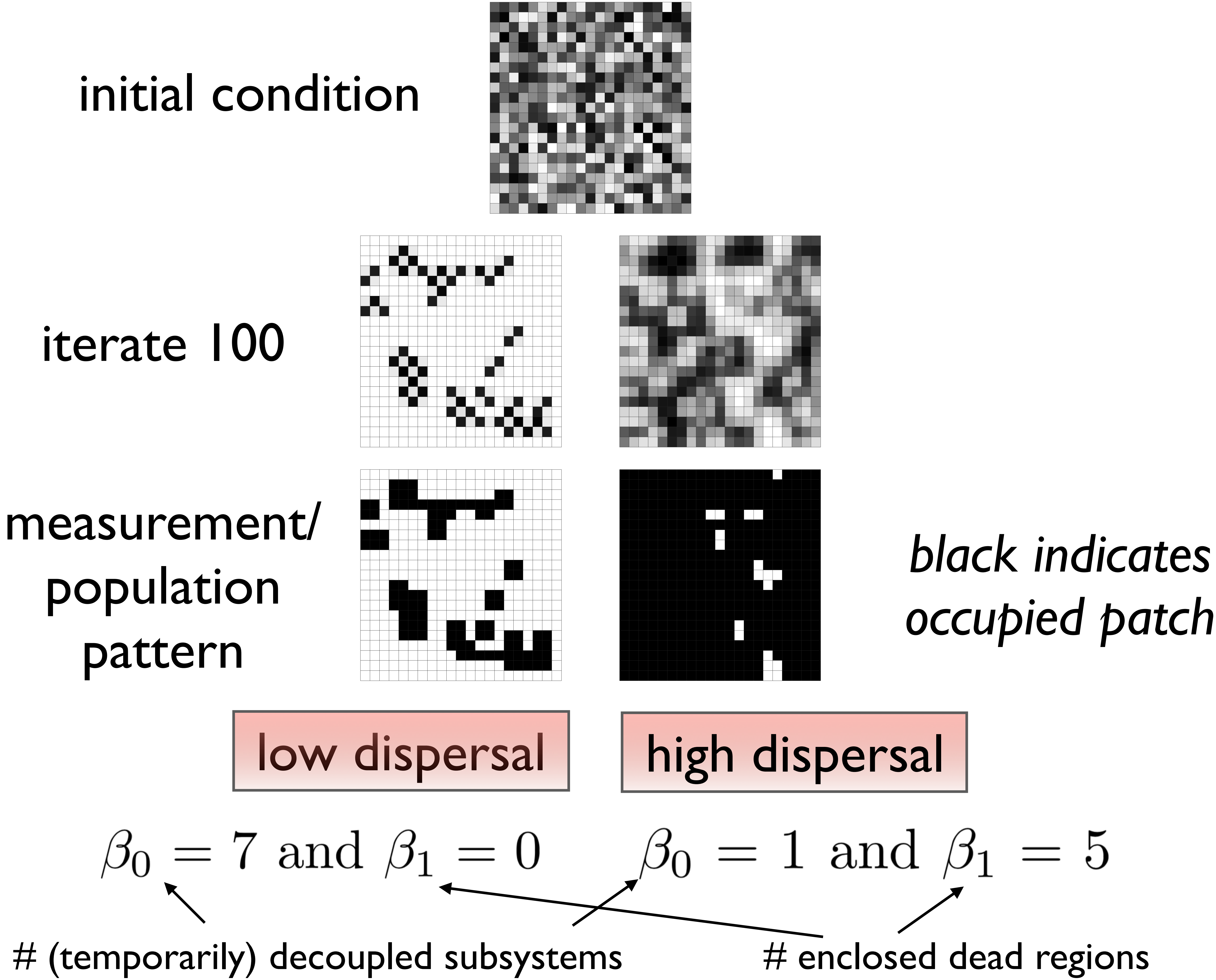
initial condition
iterate 100
measurement/ population pattern
black indicates occupied patch
low dispersal
high dispersal
$\beta_0 = 7$ and $\beta_1 = 0$
$\beta_0 = 1$ and $\beta_1 = 5$
(temporarily) decoupled subsystems
enclosed dead regions

Betti number time series

low dispersal

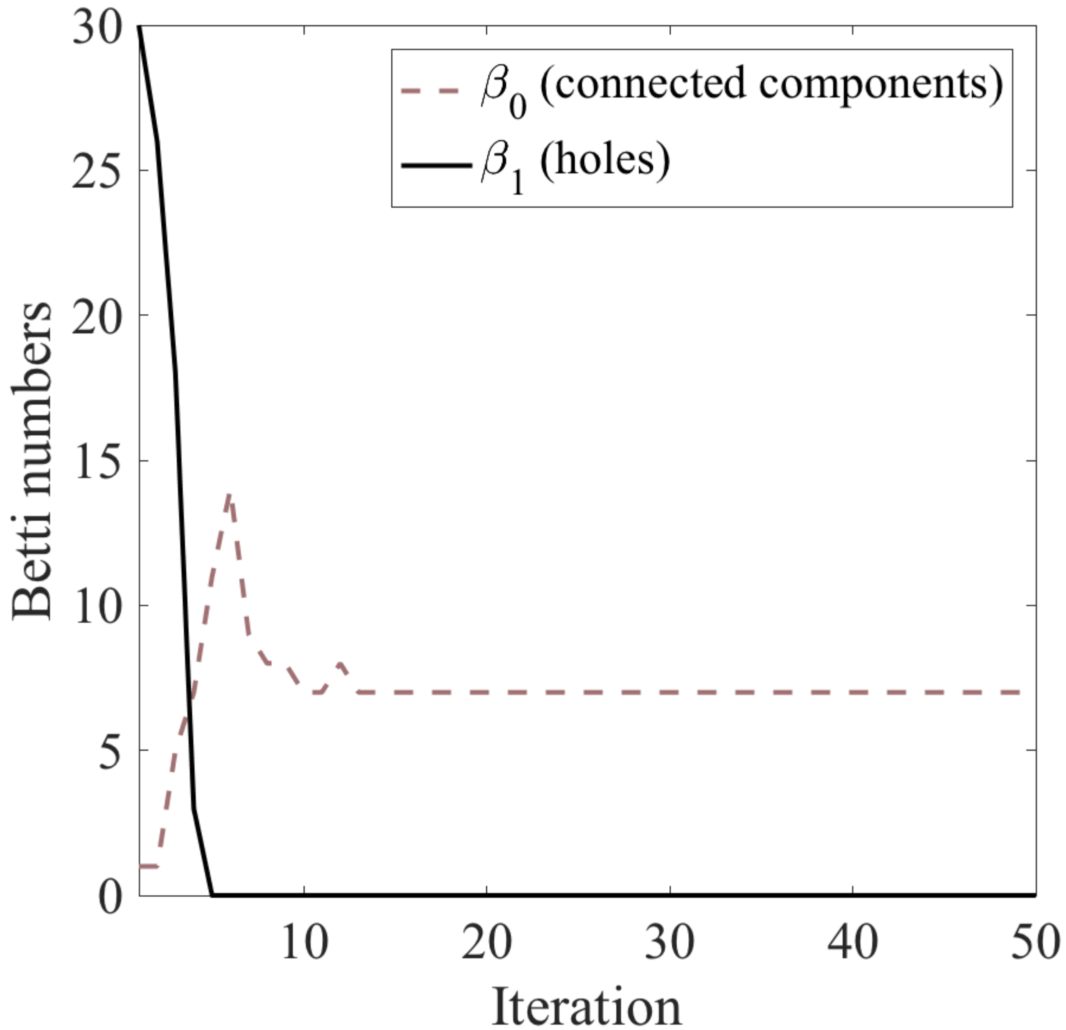

topological steady state

high dispersal

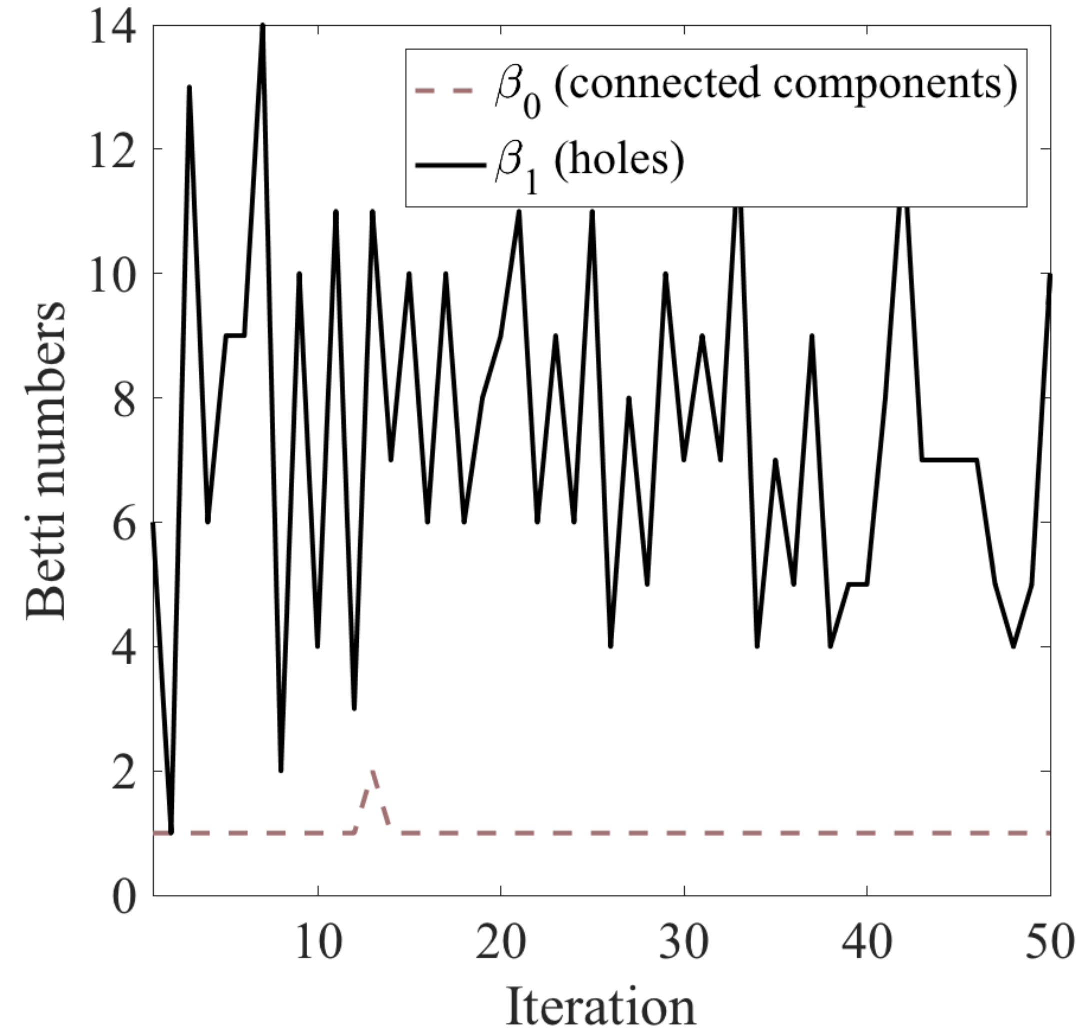

$$\chi = \sum(-1)^n k_n = \sum(-1)^n \beta_n$$

Routes to extinction

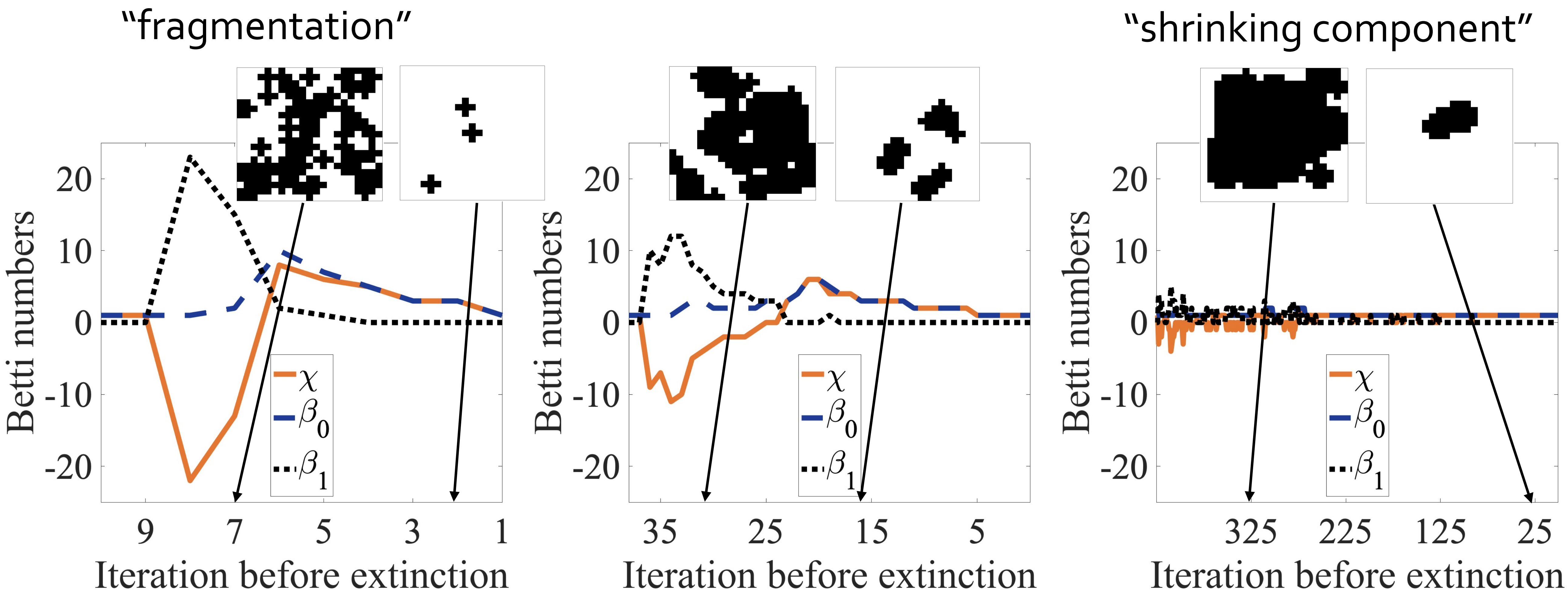

*Storch, D. *Topological early warning signals: Quantifying varying routes to extinction in a spatially distributed population model*, 2022.

Sage Stanish (WM `22, Glasgow)

THE CRITICAL TRANSITION IN THE ISING MODEL

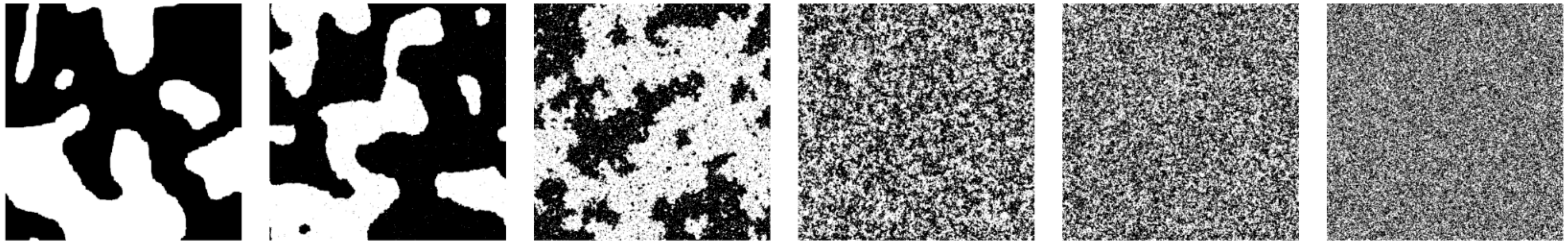

(a) $T = 0.1$ (b) $T = 0.6$ (c) $T = 1.1$ (d) $T = 1.35$ (e) $T = 1.6$ (f) $T = 2.6$

THE HOMOLOGY OF THE ISING MODEL

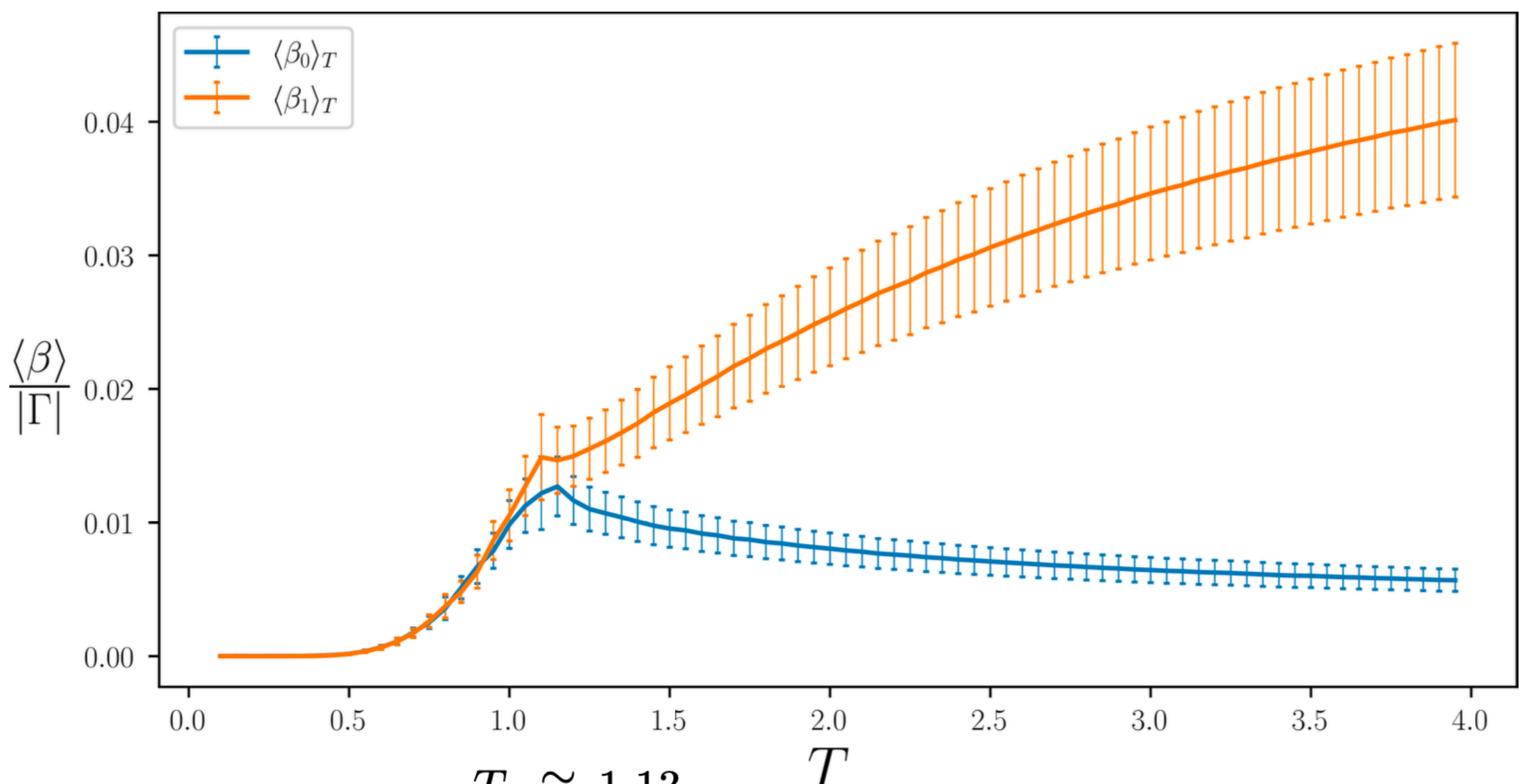

$T_c \cong 1.13$

https://i.stack.imgur.com/zWvOR.png

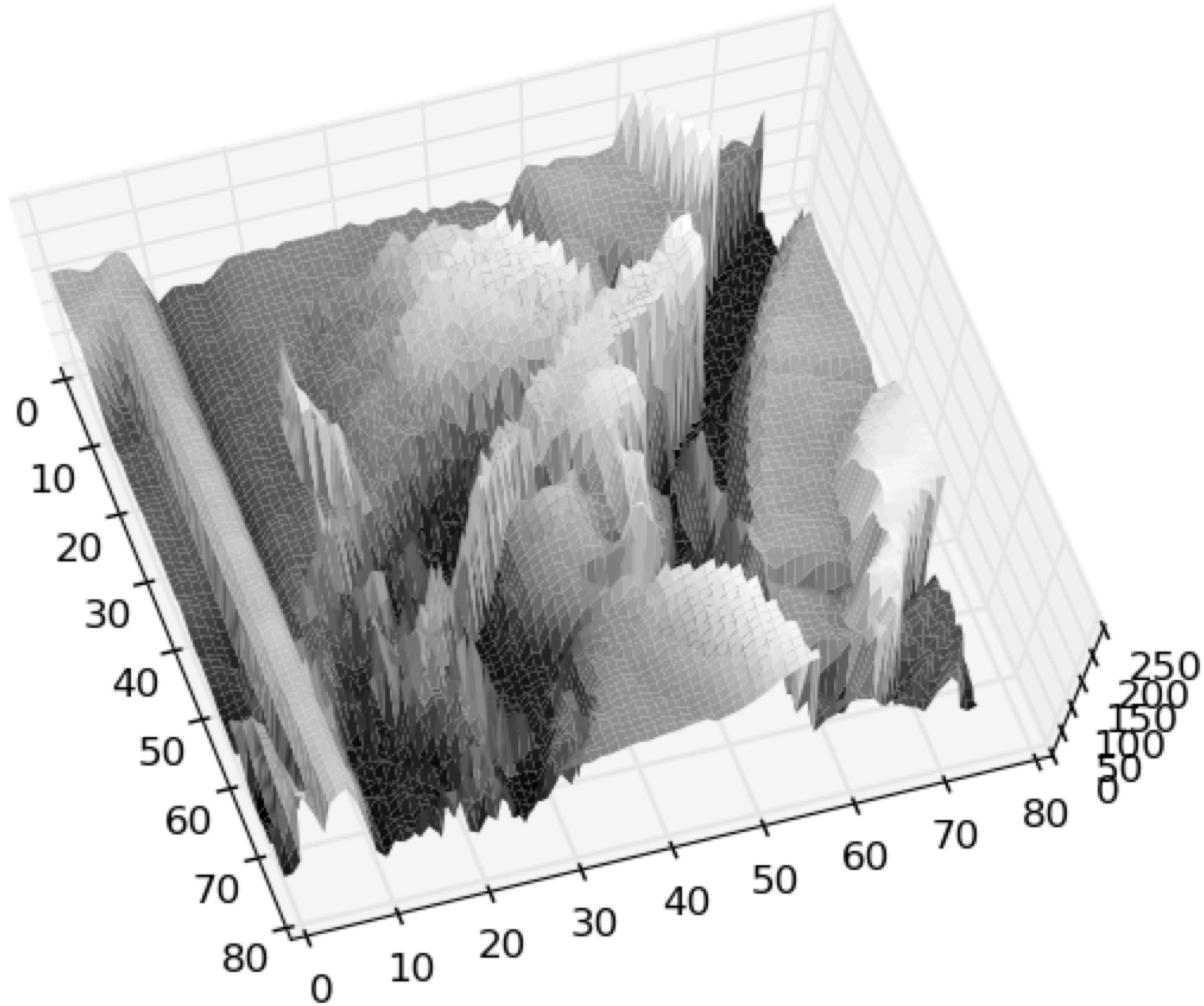

Can we use grayscale information?

Persistent Homology

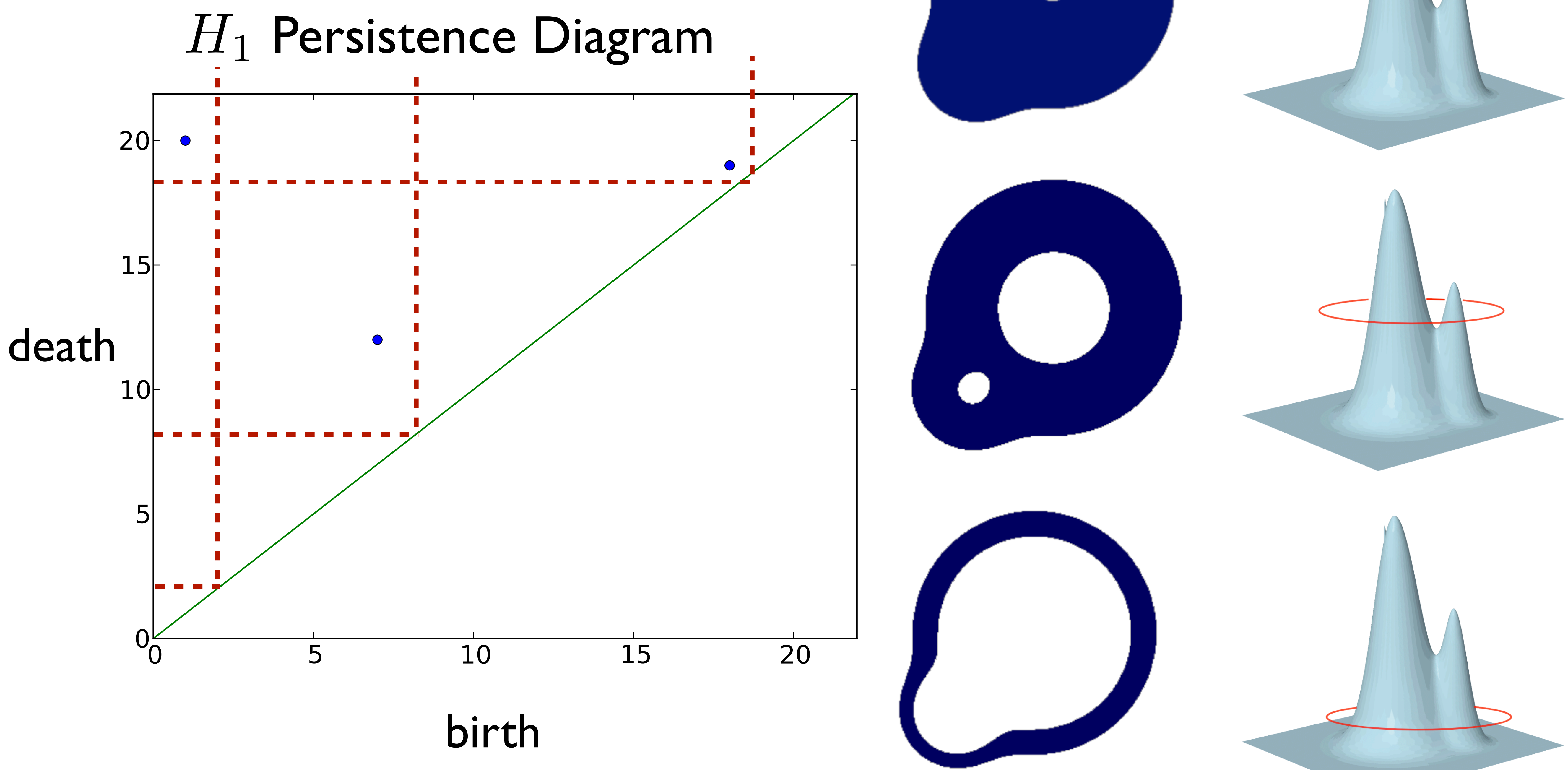

With small additive noise

H_1 Persistence Diagram

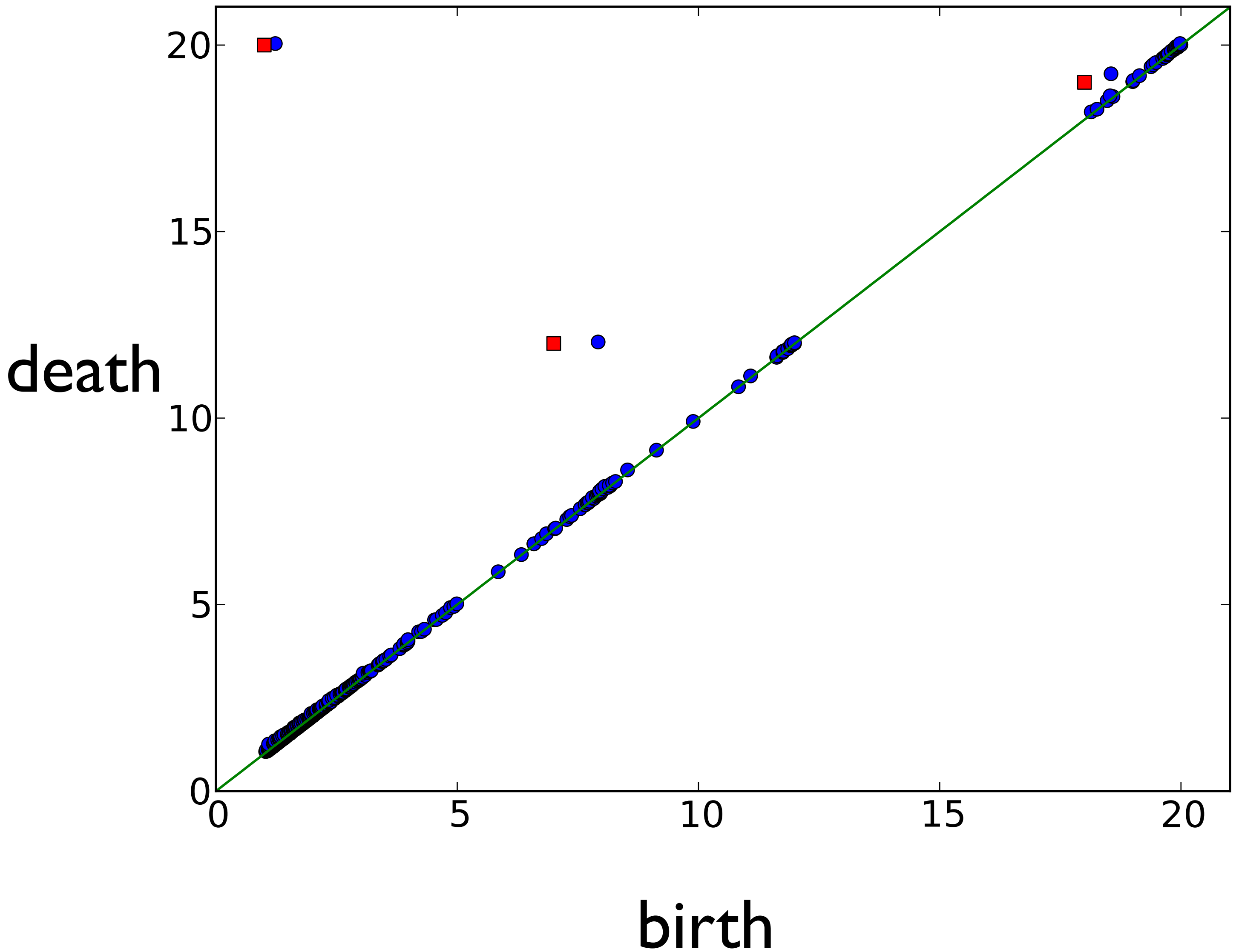

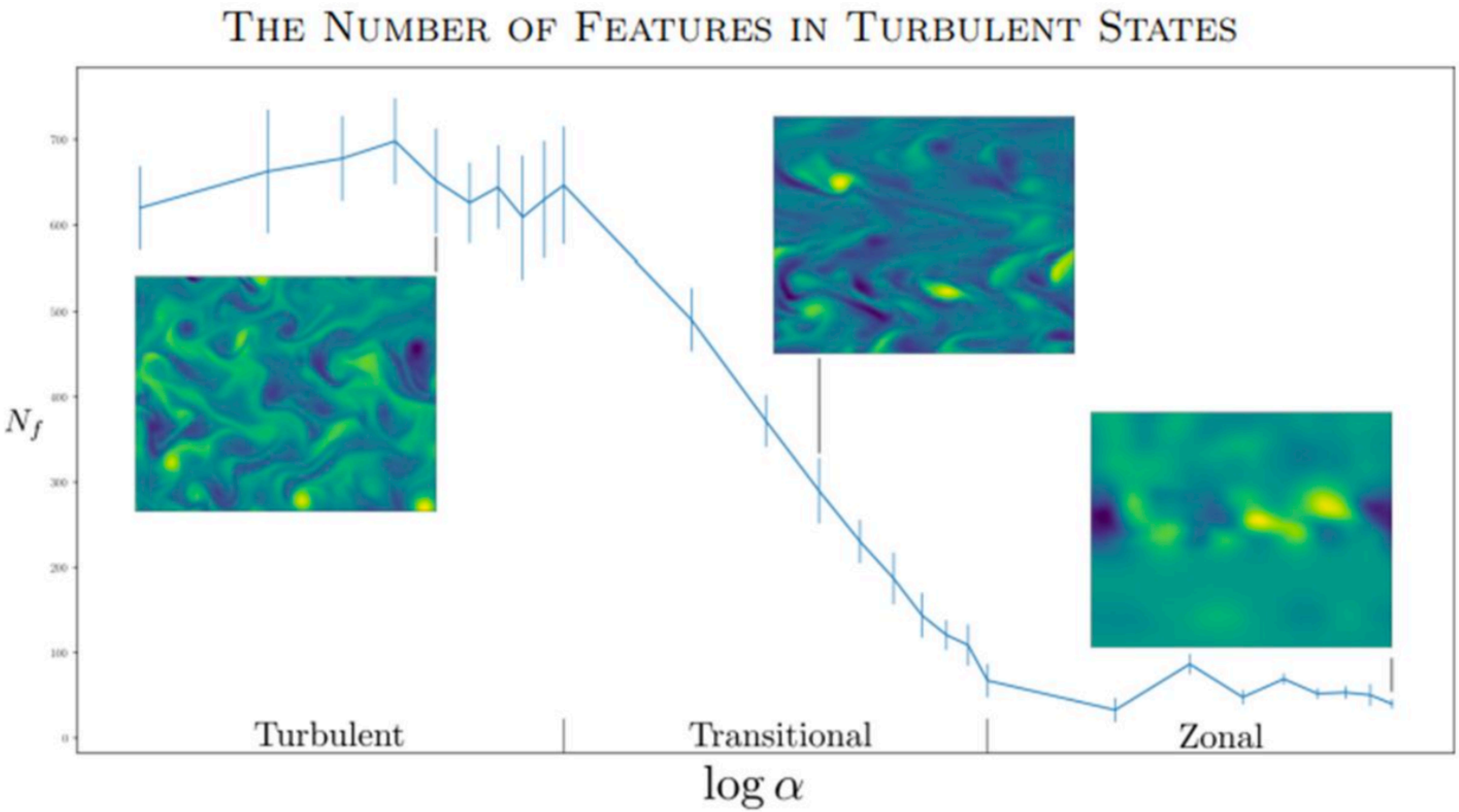

Stanish Honors Thesis `22

Coming soon … Julius Kiewel's Honors Thesis

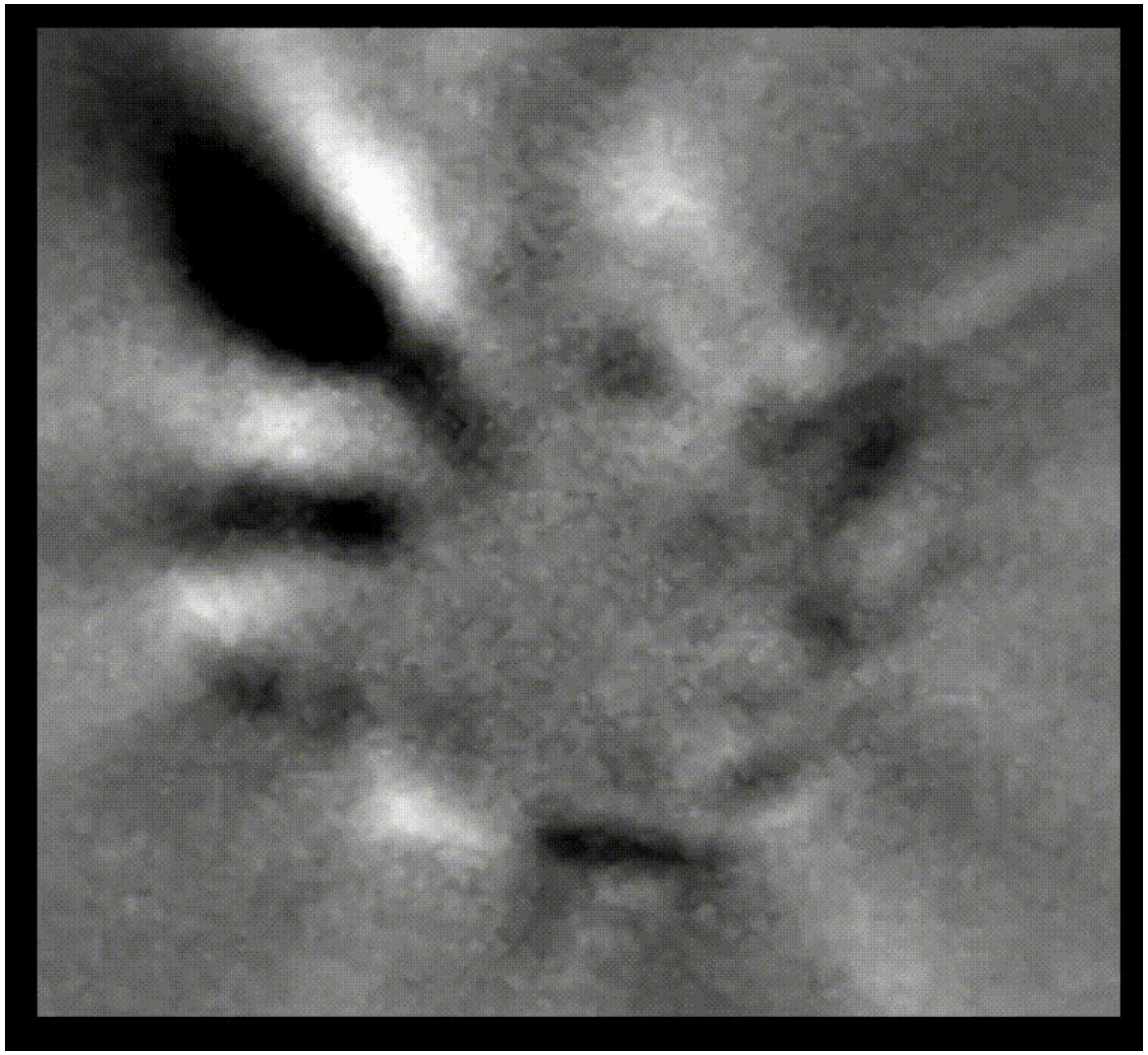

Measured Plasma

From a 1-filtration to a multi-filtration…

Definition 3 (Equations (1.6) and (1.7)[20] p. 10). *For $g \in \mathscr{I}_P$ and structuring element $B \subseteq \mathbb{Z}^m$, the erosion of g via B is an image $\varepsilon_B(g) \in \mathscr{I}_P$ defined by*

$$\varepsilon_B(g)(\mathbf{x}) = \min g\Big((\mathbf{x}+B)\cap P\Big) = \min\{g(\mathbf{x}+\mathbf{b}) \mid \mathbf{b}\in B, \mathbf{x}+\mathbf{b}\in P\}. \quad (1)$$

Similarly, the dilation of g via B is an image $\delta_B(g) \in \mathscr{I}_P$ defined by

$$\delta_B(g)(\mathbf{x}) = \max g\Big((\mathbf{x}-B)\cap P\Big) = \max\{g(\mathbf{x}-\mathbf{b}) \mid \mathbf{b}\in B, \mathbf{x}-\mathbf{b}\in P\}. \quad (2)$$

Since $\mathbf{0} \in B$ and B is finite, $(\mathbf{x}+B)\cap P$ and $(\mathbf{x}-B)\cap P$ are non-empty, finite sets whenever $\mathbf{x}\in P$. Therefore, $\varepsilon_B(g)$ and $\delta_B(g)$ are well-defined.

A shape (in blue) and its morphological dilation (in green) and erosion (in yellow) by a diamond-shaped structuring element.

By Renato Keshet - created by the user, Public Domain, https://commons.wikimedia.org/w/index.php?curid=4413072

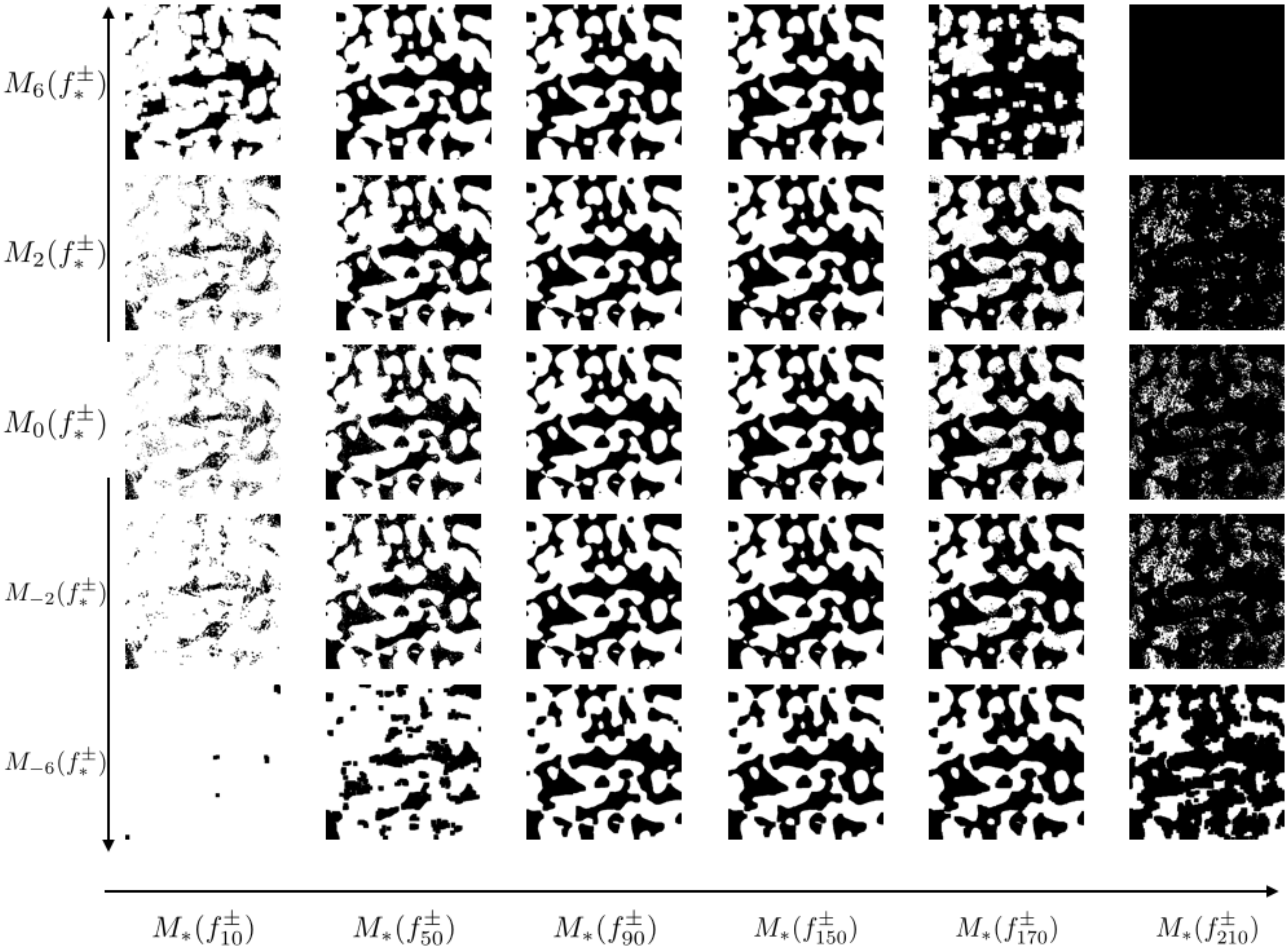

$M_6(f_*^{\pm})$
$M_2(f_*^{\pm})$
$M_0(f_*^{\pm})$
$M_{-2}(f_*^{\pm})$
$M_{-6}(f_*^{\pm})$
$M_*(f_{10}^{\pm})$
$M_*(f_{50}^{\pm})$
$M_*(f_{90}^{\pm})$
$M_*(f_{150}^{\pm})$
$M_*(f_{170}^{\pm})$
$M_*(f_{210}^{\pm})$

Set inclusions in a 2D slice of a 4-filtration…

$$
\begin{array}{ccccccc}
X^{\mathscr{E},\mathscr{D}}_{1,(n,-2,3)} & \subseteq & X^{\mathscr{E},\mathscr{D}}_{2,(n,-2,3)} & \subseteq \cdots \subseteq & X^{\mathscr{E},\mathscr{D}}_{T-1,(n,-2,3)} & \subseteq & X^{\mathscr{E},\mathscr{D}}_{T,(n,-2,3)} \\
\rotatebox{90}{$\subseteq$} & & \rotatebox{90}{$\subseteq$} & \vdots & \rotatebox{90}{$\subseteq$} & & \rotatebox{90}{$\subseteq$} \\
X^{\mathscr{E},\mathscr{D}}_{1,(n-1,-2,3)} & \subseteq & X^{\mathscr{E},\mathscr{D}}_{2,(n-1,-2,3)} & \subseteq \cdots \subseteq & X^{\mathscr{E},\mathscr{D}}_{T-1,(n-1,-2,3)} & \subseteq & X^{\mathscr{E},\mathscr{D}}_{T,(n-1,-2,3)} \\
\rotatebox{90}{$\subseteq$} & & \rotatebox{90}{$\subseteq$} & \vdots & \rotatebox{90}{$\subseteq$} & & \rotatebox{90}{$\subseteq$} \\
\vdots & & \vdots & \vdots & \vdots & & \vdots \\
\rotatebox{90}{$\subseteq$} & & \rotatebox{90}{$\subseteq$} & \vdots & \rotatebox{90}{$\subseteq$} & & \rotatebox{90}{$\subseteq$} \\
X^{\mathscr{E},\mathscr{D}}_{1,(1,-2,3)} & \subseteq & X^{\mathscr{E},\mathscr{D}}_{2,(1,-2,3)} & \subseteq \cdots \subseteq & X^{\mathscr{E},\mathscr{D}}_{T-1,(1,-2,3)} & \subseteq & X^{\mathscr{E},\mathscr{D}}_{T,(1,-2,3)} \\
\rotatebox{90}{$\subseteq$} & & \rotatebox{90}{$\subseteq$} & \vdots & \rotatebox{90}{$\subseteq$} & & \rotatebox{90}{$\subseteq$} \\
X^{\mathscr{E},\mathscr{D}}_{1,(0,-2,3)} & \subseteq & X^{\mathscr{E},\mathscr{D}}_{2,(0,-2,3)} & \subseteq \cdots \subseteq & X^{\mathscr{E},\mathscr{D}}_{T-1,(0,-2,3)} & \subseteq & X^{\mathscr{E},\mathscr{D}}_{T,(0,-2,3)}
\end{array}
$$

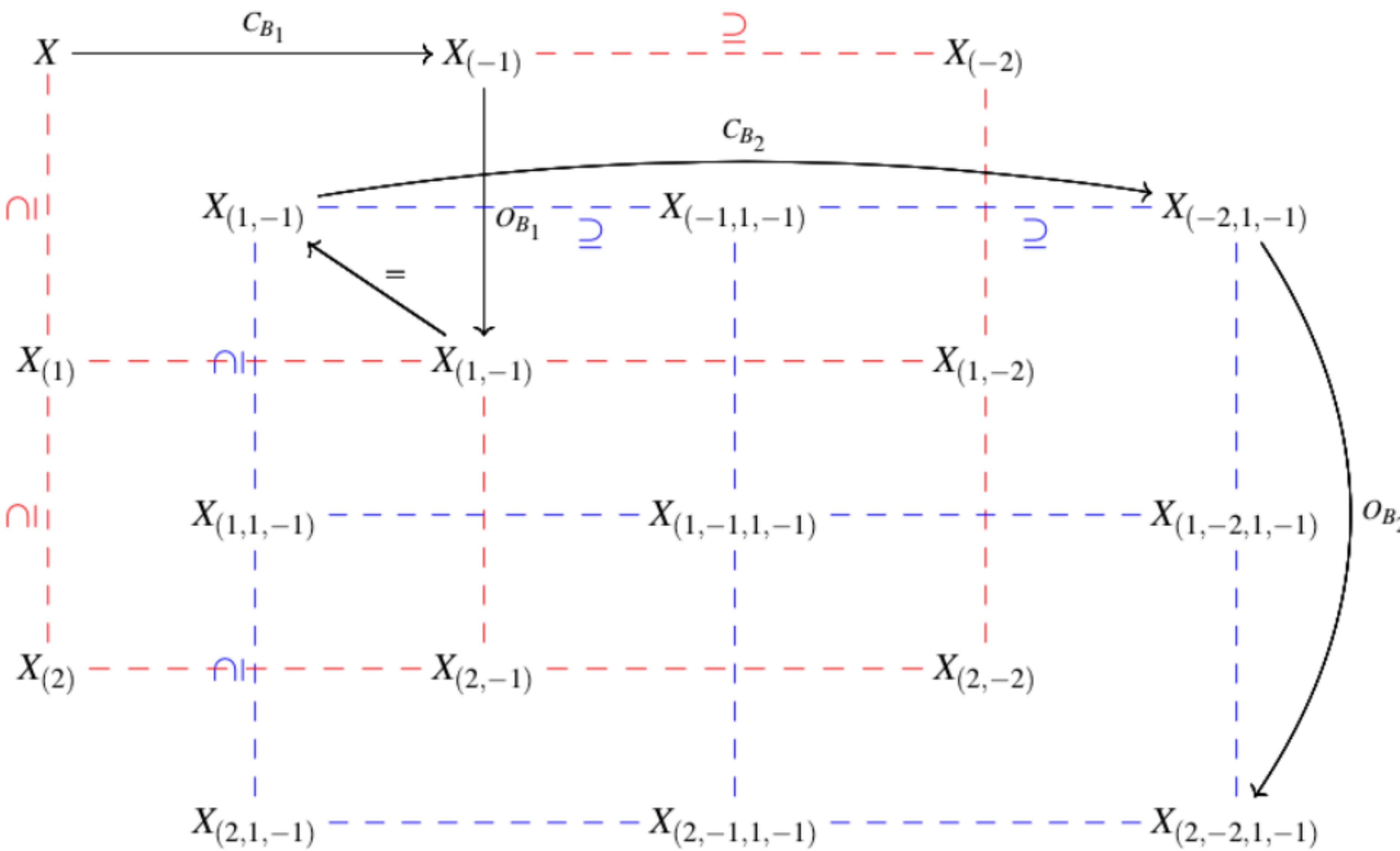



*Chung, Day, Hu. *A Multiparameter Persistence Framework for Mathematical Morphology*, submitted 2021.

Zooming out . . .

- More techniques are needed to extract information from morphological/thresholding multifiltrations.

- *These techniques may be able to overcome problems of error, noise, and missingness/sparsity in spatial data.*

- There are similar TDA tools to study point cloud and graph/network structure.

- Yet more sophisticated techniques (filtrations and invariants) may be used to track dynamics.

Thank you!